

Color Image Encryption Scheme Based On Alternate Quantum Walk and Controlled Rubik's Cube

Jingbo Zhao

Qingdao University of Technology

Tian Zhang

Qingdao University of Technology

Jianwei Jiang

Qingdao University of Technology

Tong Fang

Qingdao University of Technology

Hongyang Ma (✉ ma@aliyun.com)

Qingdao University of Technology

Research Article

Keywords: intercepted, transmission, encryption, whirling, simulation

Posted Date: January 3rd, 2022

DOI: <https://doi.org/10.21203/rs.3.rs-1204955/v1>

License:   This work is licensed under a Creative Commons Attribution 4.0 International License.

[Read Full License](#)

Color image encryption scheme based on alternate quantum walk and controlled Rubik's Cube

Jingbo Zhao¹, Tian Zhang¹, Jianwei Jiang^{1,+}, Tong Fang^{1,+}, and Hongyang Ma^{2,*}

¹School of Information and Control Engineering, Qingdao University of Technology, Qingdao, 266000, China

²School of Science, Qingdao University of Technology, Qingdao, 266000, China

*hongyang_ma@aliyun.com

+these authors contributed equally to this work

ABSTRACT

Aiming at solving the trouble that digital image information is easily intercepted and tampered during transmission, we proposed a color image encryption scheme based on alternate quantum random walk and controlled Rubik's Cube transformation. At the first, the color image is separated into three channels: channel R, channel G and channel B. Besides, a random sequence is generated by alternate quantum walk. Then the six faces of the Rubik's Cube are decomposed and arranged in a specific order on a two-dimensional plane, and each pixel of the image is randomly mapped to the Rubik's Cube. The whirling of the Rubik's Cube is controlled by a random sequence to realize image scrambling and encryption. The scrambled image acquired by Rubik's Cube whirling and the random sequence received by alternate quantum walk are bitwise-XORed to obtain a single-channel encrypted image. Finally the three-channel image is merged to acquire the final encrypted image. The decryption procedure is the reverse procedure of the encryption procedure. The key space of this scheme is theoretically infinite. After simulation experiments, the information entropy after encryption reaches 7.999, the NPCR is 99.5978%, and the UACI is 33.4317%. The encryption scheme with high robustness and security has an excellent encryption effect which is effective to resist statistical attacks, force attacks, and other differential attacks.

1 Introduction

As multimedia technology is growing well today, an increasing number of fields are gradually developing in the direction of digitization and informatization, which has brought convenience to our lives and work. However, the security and confidentiality of data in the process of information transmission are becoming more and more important image plays. As one of the important carriers in the process of information transmission, digital images play a pivotal role in many fields, such as education, finance, medical treatment and so on. However, digital images are easily intercepted and tampered during transmission, which greatly threatens the privacy of image information¹⁻⁴. In view of the security of digital images, many domestic and foreign researchers have brought forward various image encryption methods. For example, digital image encryption schemes are based on chaotic systems⁵⁻⁸, which control the placement of image pixels by generating random sequences through the chaotic system. Based on digital image encryption schemes such as Fourier Transform^{9,10}, the image is transformed into the frequency domain, and then the amplitude value of the sine and cosine function of each frequency in the frequency domain is operated to realize image encryption; there are also classical digital image encryption methods, such as: Arnold transformation¹¹⁻¹⁴, AES transformation¹⁵⁻¹⁸, DNA encoding encryption¹⁹⁻²⁴, etc. Based on the alternate quantum random walk and controlled Rubik's Cube transform, this paper comes up with a novel digital image encryption scheme.

With the continuous development of quantum computing and quantum communication, many quantum algorithms and quantum technologies have emerged²⁵⁻³³. Quantum random walk is generated by applying classical random walk to quantum computing, and it plays an important part in a number of quantum algorithms³⁴⁻³⁷. Compared with classical random walking, quantum random walk has two main advantages, one is fast running speed, and the other is strong security. Similar to chaotic systems, quantum random walk has many excellent properties: sensitivity to initial values, stability, non-periodicity, etc. Thence, the key space of quantum random walk is very vast, and it has a perfect capability to resist external malicious attacks. Therefore, quantum random walk is very advantageous in the field of image encryption. Wang et al. designed an image encryption algorithm that combines quantum random walk with DNA encoding¹⁹. Based on quantum random walk and double random phase encoding technology, Abd-El-Atty et al. put forward an image encryption scheme³⁸. MA et al. designed an image encryption scheme that combines alternating quantum random walk with discrete cosine transform¹.

The principle of Rubik's Cube transformation is inspired by Rubik's Cube. The Rubik's Cube is to change the position of the sub-block by moving the sub-blocks, so as to realize the scrambling of the Rubik's Cube. Similarly, applying the Rubik's Cube transformation to image scrambling is to scramble the image by moving the position of the image pixels³⁹⁻⁴³. For a

third-order Rubik's Cube, if a certain layer is rotated 90 degrees at a time, there are eighteen ways for rotation. There are several ways of permutation and combination of a 3rd-order Rubik's Cube, but it is the only way to restore, so the computational complexity is very high. Thus it is feasible to combine the Rubik's Cube transformation with the image encryption. Zhang et al. proposed an image encryption scheme based on Rubik's Cube transformation and chaotic sequence⁴⁰. Loukhaoukha et al. designed an image encryption method based on the Rubik's Cube rotation principle⁴². At first, the original image was scrambled by using the Rubik's Cube principle, and then the rows and columns of the scrambled image were XORed with the key. Vidhya et al. designed a chaotic image encryption algorithm based on Rubik's Cube transformation and prime number decomposition algorithm⁴³.

This article combines quantum random walk with Rubik's Cube transformation to complete the encryption of digital images. Firstly, a random sequence is generated by quantum walking. Then the random sequence is used to control the magic cube transform to achieve the purpose of image scrambling. The full text of this article is structured as follows: The second part introduces the relevant knowledge needed in the paper. Next part introduces the principles and processes of image encryption and decryption. The Fourth part presents the simulation results and the analysis of the simulation results. Finally, we draw a conclusion about the scheme.

2 Principle

2.1 Alternate quantum walks

Quantum walk can be separated into two parts: One is discrete time quantum random walk and the other is continuous time quantum random walk. We focus on the former way of random walking in this paper.

Similar to the classic random walk, quantum walk is mainly composed of coin register (coin space \mathcal{H}^c) and Rambler location information (Rambler's location space \mathcal{H}^l). Therefore, the quantum walk is carried out in Hilbert space $\mathcal{H} = \mathcal{H}^c \otimes \mathcal{H}^l$. The process of quantum random walk is separated into two steps. The first step is to apply the coin operator on the coin state of the two-dimensional Hilbert space \mathcal{H}^c , and then apply the unitary operator \hat{U} to the total Hilbert space \mathcal{H} . Thus the quantum also can be seen as the application of a unitary operator U that acts repeatedly on the quantum walk system and the operator can be described as:

$$\hat{U} = SC = S(\hat{C} \otimes I) \quad (1)$$

Assume that the quantum walk coin operator always chooses the same operator \hat{C} :

$$\hat{C} = \begin{pmatrix} \cos \alpha & \sin \alpha \\ -\sin \alpha & \cos \alpha \end{pmatrix} \quad (2)$$

when $\alpha = \frac{\pi}{4}$, the coin operator can be expressed as:

$$\hat{C} = \frac{\sqrt{2}}{2} \begin{pmatrix} 1 & 1 \\ -1 & 1 \end{pmatrix} = H \quad (3)$$

The transfer operator S is used in quantum walks to manipulate the walker to decide the direction of the next walk. When the condition of coin state is $|0\rangle$ (spin up $|\uparrow\rangle$), the walker will move forward in a certain direction. While the condition of coin state is $|1\rangle$ (spin down $|\downarrow\rangle$), the walker will take one step further in the opposite direction. So the transfer operator \mathcal{S} can be denoted as:

$$S = |0\rangle\langle 0| \otimes |n+1\rangle\langle n| + |1\rangle\langle 1| \otimes |n-1\rangle\langle n| \quad (4)$$

In the alternate quantum walk, it is formed by the position state tensor $\{|x, y\rangle, x, y \in Z\}$, walking alternately in two directions in a two-dimensional space. Therefore, in the quantum random walk process, the unitary operator repeatedly acting on the quantum walk system can be denoted as:

$$\hat{U} = \hat{S}_y(I \otimes \hat{C})\hat{S}_x(I \otimes \bar{C}) = \hat{S}_y(I \otimes H)\hat{S}_x(I \otimes H) \quad (5)$$

$$\begin{aligned} \hat{S}_y &= |0\rangle\langle 0| \otimes \sum_{m,n \in Z} |n+1, m\rangle\langle n, m| \\ &+ |1\rangle\langle 1| \otimes \sum_{m,n \in Z} |n-1, m\rangle\langle n, m| \end{aligned} \quad (6)$$

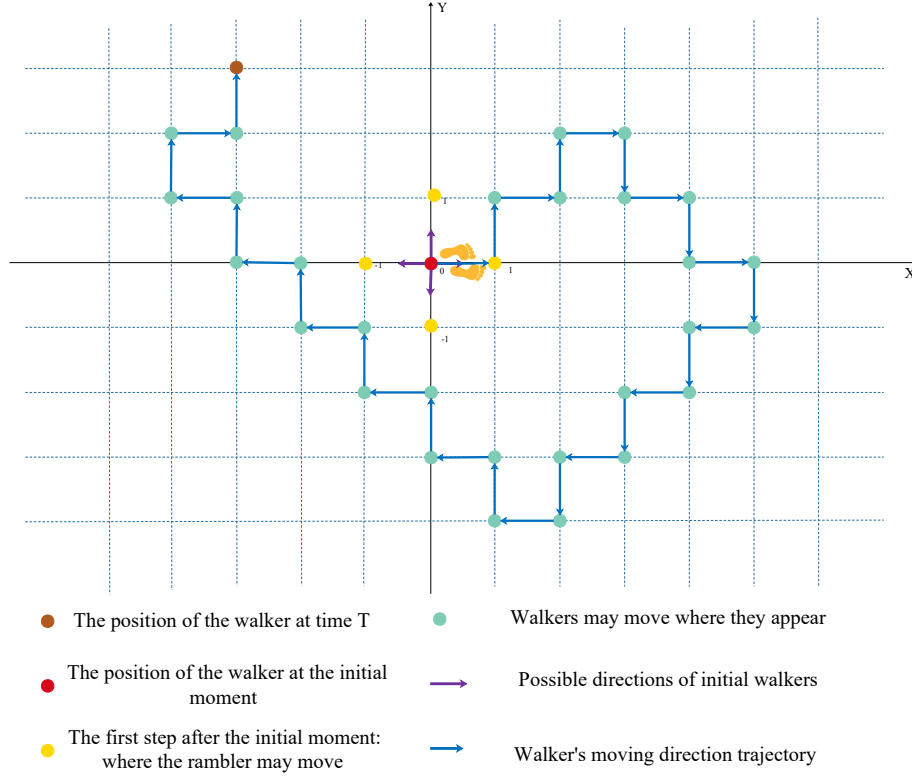


Figure 1. Alternate quantum walk.

$$\begin{aligned}
 \hat{S}_x = & |0\rangle\langle 0| \otimes \sum_{m,n \in \mathbb{Z}} |n, m+1\rangle\langle n, m| \\
 & + |1\rangle\langle 1| \otimes \sum_{m,n \in \mathbb{Z}} |n, m-1\rangle\langle n, m|
 \end{aligned} \tag{7}$$

When the coin state is $|0\rangle$ ($|1\rangle$), act on the walker to walk up (down) along the Y axis, and act on the walker to make it walk right (to the left) along the X axis as shown in Fig. 1. Assuming that the walker is locally at the initial moment $(y, x) = (0, 0)$, the initial state of the coin state is a superposition state $|\text{coin}\rangle = a|0\rangle + b|1\rangle$, and the quantum state of the initial quantum walk can be expressed as: $|\psi_0\rangle = |00\rangle \otimes |\text{coin}\rangle$. Here, after walking N steps, the final quantum state of the entire system is $|\psi_N\rangle = \hat{U}^N |\psi_0\rangle$. The probability that the walker is at the location (y, x) is:

$$P_{Y,X} = \sum |\langle y, x, 0 | \hat{U}^N | \psi_0 \rangle|^2 + \sum |\langle y, x, 1 | \hat{U}^N | \psi_0 \rangle|^2 \tag{8}$$

2.2 Rubik's Cube Transform

The concept of Rubik's Cube transformation comes from Rubik's Cube toys, which disrupt the patterns on the surface of the Rubik's Cube by rotating the cubes. The algorithm in this paper is based on the third-order Rubik's Cube. The third-order Rubik's Cube is a special cube that is composed of 26 sub-blocks and can be rotated along each axis. The six faces of the Rubik's Cube have different colors.

For a 3rd-order Rubik's Cube, we firstly determine the representation of the 6 faces of the Rubik's Cube, and mark each sub-block of the Rubik's Cube. Third-order Rubik's Cube expansion map is displayed in Fig. 2, the top side is represented as U, the front side is represented as F, the right side is represented as R, the bottom side is represented as D, the back side is represented as B, and the left side is represented as L. Because U surface and D surface, R surface and L surface, and F surface and B surface are relative, we only consider the three surfaces: U, R, and F. For example, when the first layer of the U side of the Rubik's Cube is rotated 90 degrees to the right, the state of the Rubik's Cube is demonstrated in Fig. 2. And the U surface is rotated 90 degrees counterclockwise, while the D surface does not change. When the middle layer of the U side of the Rubik's Cube is rotated 90 degrees, the middle layers of the four sides of F, R, B, and L are also cyclically shifted, while the U and D surfaces do not change. Similarly, the same principle applies to rotating other surfaces.

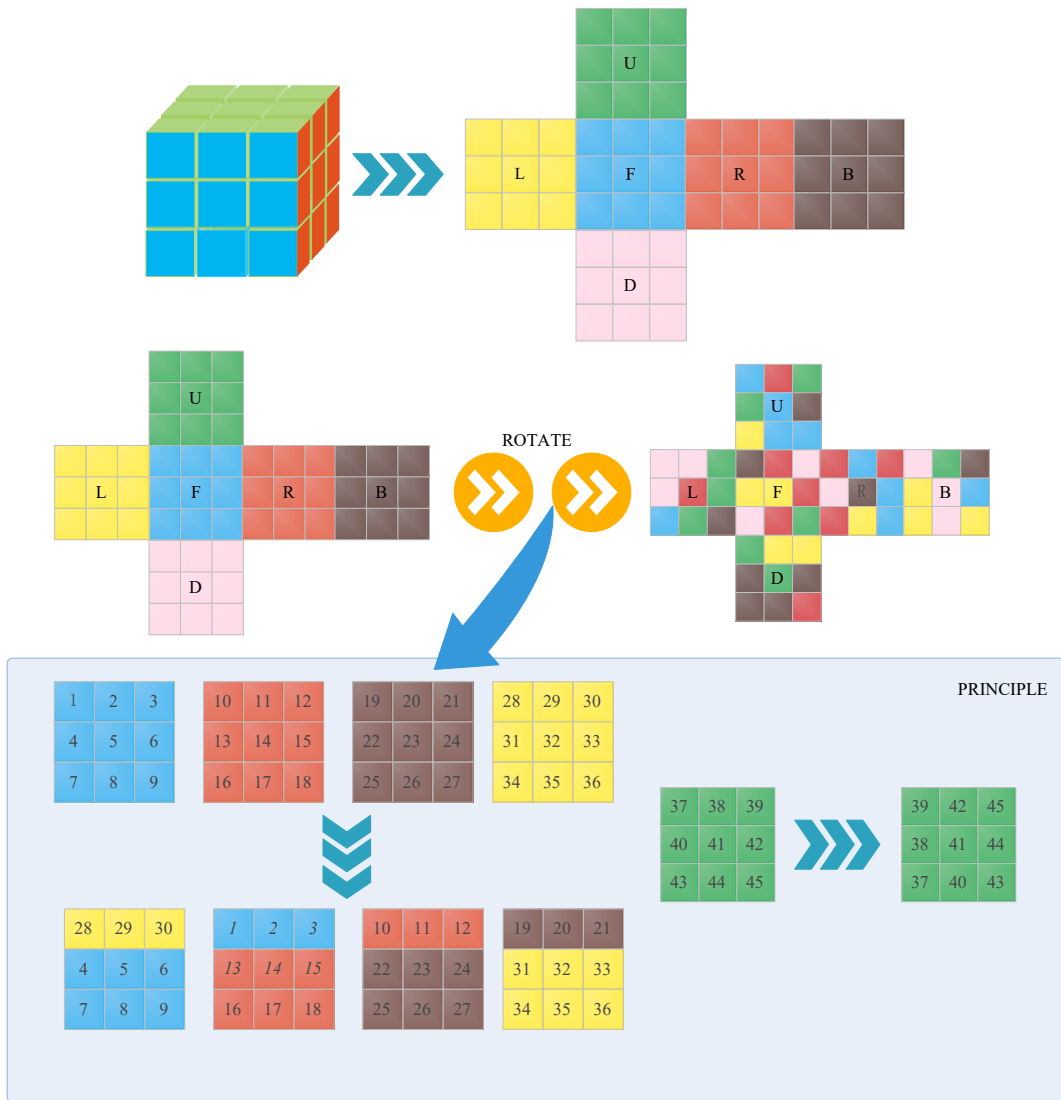


Figure 2. Third-order Rubik's Cube principle. The upper part is the expansion diagram of the Rubik's Cube, the middle is the Rubik's Cube rotation, and the lower layer is the basic Rubik's Cube rotation principle.

Through the above principles, rotating the Rubik's Cube can be pieced together into a specific pattern, or the specific pattern can be messed up. We apply the theory of Rubik's Cube transformation to image encryption. The pixels of the image are mapped to the Rubik's Cube, and a sub-block of the Rubik's Cube is regarded as a pixel on the image. According to the principle of Rubik's Cube transformation and a specific whirling rule, the pixel position of the original image is shuffled to generate an irregular image. The recipient can use the key to decrypt the encrypted image to acquire the original image. Therefore, the privacy and security of image information in the transmission process can be improved.

3 Principle of Encryption and Decryption

In this paper, a random probability matrix is generated by alternating quantum walks and transformed an one-dimensional sequence, the rotation of the Rubik's Cube is controlled by this sequence. Through rotation, the scrambling image is XORed with the matrix converted from the random probability matrix to obtain the encrypted image.

3.1 Encryption Algorithm

The random sequence can be obtained through quantum walk, which makes the image difficult to be eavesdropped on. Therefore the scheme has good security. The detailed steps of the encryption algorithm are as follows (Fig. 3 is the encryption flowchart):

Step1: Enter the image \mathcal{I} to be encrypted, analyze the image information, especially the size information $\mathcal{I}(m, n, 3)$. Split

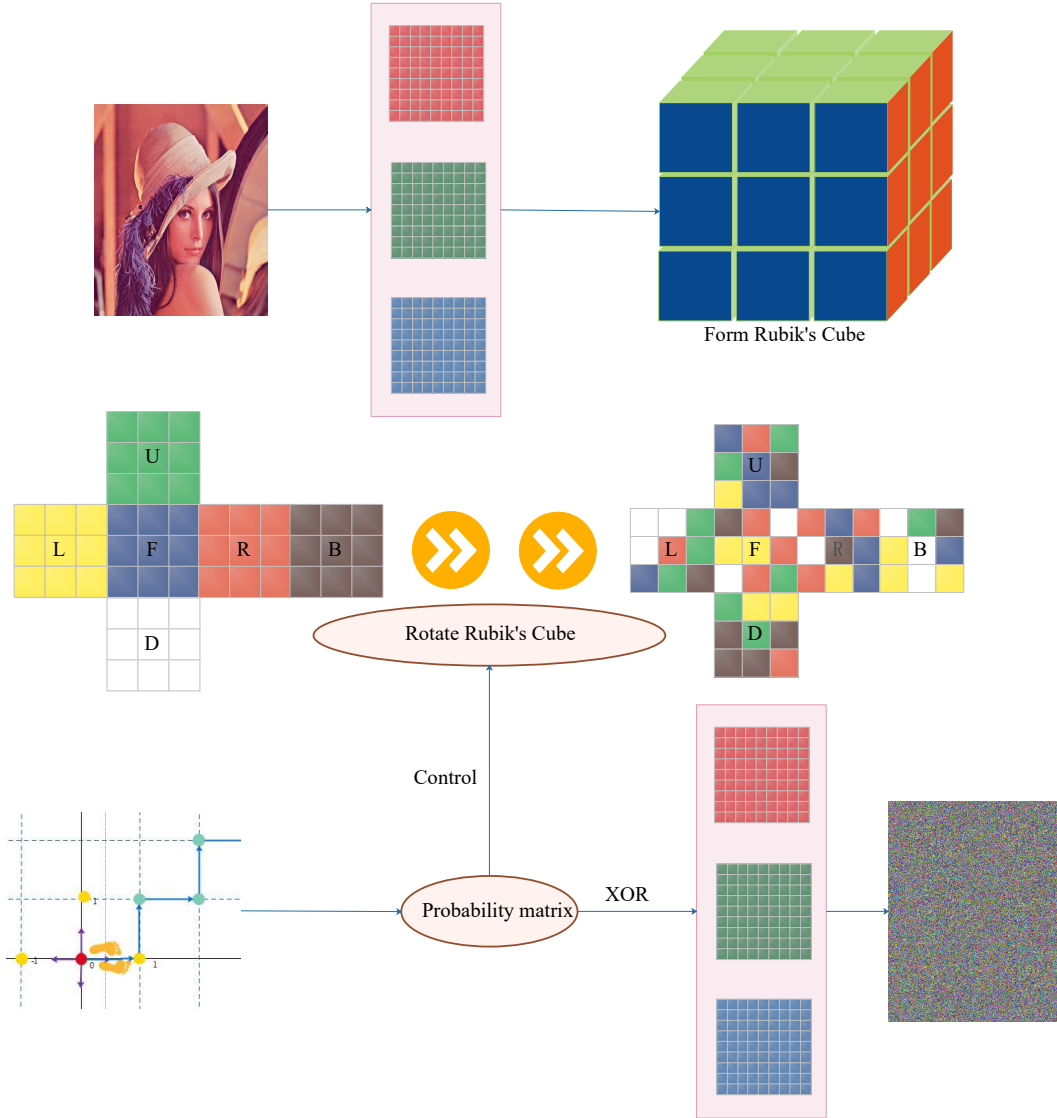


Figure 3. Encryption flowchart. Separate the three channels, select pixels to form a Rubik's Cube, use alternate quantum walks to control the Rubik's cube rotation, scramble and encrypt, merge the three channels to get an encrypted image.

the original color image $\mathcal{I}(m, n, 3)$ into $\mathcal{R}(m, n)$, $\mathcal{G}(m, n)$, $\mathcal{B}(m, n)$ three-channel images and represent them in a pixel matrix:

$$\mathcal{I}(m, n, 3) = [\mathcal{R}(m, n), \mathcal{G}(m, n), \mathcal{B}(m, n)] \quad (9)$$

Step2: Select the parameters (N_1, N_2, a, b) of the alternate quantum walk, walk \mathcal{N} steps on the initial state ψ_0 , and generate a probability distribution matrix: $P_{y,x}$ of size (m, n) :

$$P_{Y,X} = \sum |\langle y, x, 0 | \hat{U}^N | \psi_0 \rangle|^2 + \sum |\langle y, x, 1 | \hat{U}^N | \psi_0 \rangle|^2 \quad (10)$$

Step3: Divide the single-channel image into 6 parts without superimposition to obtain 6 sub-images of different matrices, and treat the 6 matrices as 6 faces of the Rubik's Cube-front (F), back (B), and top (U), Bottom surface (D), left side (L), right side (R):

$$I = (F, B, U, D, L, R) \quad (11)$$

Step4: Take out the 3×3 pixel matrix from the 6 matrices to form 6 faces and form a 3rd-order cube, and the surface has 54 pixel values, so the image can produce a cube.

Table 1. Third-order Rubik's Cube Rotation.

Method	Direction	Affected four faces	Surface affected by rotation
U1	Clockwise	F R B L	U
U2	Clockwise	F R B L	NULL
U3	Clockwise	F R B L	D
L1	Clockwise	F D B U	L
L2	Clockwise	F D B U	NULL
L3	Clockwise	F D B U	R
F	Clockwise	U R B L	F
F2	Clockwise	U R B L	NULL
F3	Clockwise	U R B L	B
U1'	Counterclockwise	F R B L	U
U2'	Counterclockwise	F R B L	NULL
U3'	Counterclockwise	F R B L	D
L1'	Counterclockwise	F D B U	L
L2'	Counterclockwise	F D B U	NULL
L3'	Counterclockwise	F D B U	R
F1'	Counterclockwise	U R B L	F
F2'	Counterclockwise	U R B L	NULL
F3'	Counterclockwise	U R B L	B

U1: Rotate the first layer from top to bottom. U2: Rotate the second layer from top to bottom. U3: Rotate the third layer from top to bottom. L1: Rotate the first layer from left to right. L2: Rotate the second layer from left to right. L3: Rotate the third layer from left to right. F1: Rotate the first layer from front to back. F2: Rotate the second layer from front to back. F3': Rotate the third layer from front to back. U1': Rotate the first layer from top to bottom. U2': Rotate the second layer from top to bottom. U3': Rotate the third layer from top to bottom. L1': Rotate the first layer from left to right. L2': Rotate the second layer from left to right. L3': Rotate the third layer from left to right. F1': Rotate the first layer from front to back. F2': Rotate the second layer from front to back. F3': Rotate the third layer from front to back.

Step5: Obtain the random probability matrix $P_{y,x}$ through the discrete time alternate quantum walk, and convert it to an integer value of [0-17] and use it to represent the rotation method as shown in table 1:

$$K = \text{fix}(P_{y,x} \times 10^{16}) \bmod 18 \quad (12)$$

Step6: Rotating the Rubik's Cube, dividing the sequence obtained in discrete time into 6 parts, each part corresponds to a different Rubik's cube rotation mode, and the set K of integer value is [0-17] representing 18 rotation modes \mathcal{R}_{ot} .

Step7: Rotate each face element of the Rubik's cube that has just been rotated firstly by row and bitwise right circularly shifted by the value of K, and then circularly shifted bitwise right by column by the value of K:

$$K = \text{fix}(P_{y,x} \times 10^{16}) \bmod 18 \quad (13)$$

Step8: Convert the random matrix $P_{y,x}$ to an integer matrix of [0-255]: $L = \text{fix}(P_{y,x} \times 10^{16}) \bmod 256$, and then react to the third step, and perform bitwise XOR processing with rotated matrix to obtain a single-channel encrypted image.

$$I_{en} = I_1 \oplus L = I_1 \oplus [\text{fix}(P_{y,x} \times 10^{16}) \bmod 256] \quad (14)$$

Step9: Perform the same steps above for three channels, combine the encrypted three channel image of R, G, and B to obtain a color encrypted image.

3.2 Decryption Algorithm

Decryption is the contrary procedure of encryption. Briefly describe the decryption process.

Step1: Split the encrypted color image into R, G, and B three-channel images to obtain three single-channel encrypted images.

Step2: Use the parameters selected in the encryption process to perform a discrete time alternate quantum walk, generate a matrix, convert it into a pixel value matrix of [0-255], and take bitwise XOR with the encrypted image

Step3: Divide the image matrix into 6 parts and the sequence obtained in discrete time is divided into 6 parts.

Step4: Convert the probability matrix $P_{y,x}$ to the integer sequence value of [0-17], and perform the Rubik's Cube reduction based on this.

$$\begin{cases} k' = k + 3, k \in (0, 1, 2, 6, 7, 8, 12, 13, 14) \\ k' = k - 3, k \in (3, 4, 5, 9, 10, 11, 15, 16, 17) \end{cases} \quad (15)$$

Step5: Apply step 3 in the reverse direction, merge the sub-images into a single-channel image of size, and then merge the decrypted three channel image to obtain the original image.

4 Experiments and Performance Analysis

So as to prove that the proposed encryption scheme has sufficient security, we select 4 color images with size of 512*512 for simulation analysis. This section analyzes the histogram, correlation, information entropy, key space, key sensitivity, and PSNR of encrypted images. The parameters of the alternate quantum walk generation key are $(512, 512, \frac{\pi}{2}, \frac{\pi}{3})$.

4.1 Encryption Effect

We choose three color images to perform a simulation, and the results are demonstrated in Fig.4. From the Fig.4, it's obvious that the encrypted image has no visual information about original image.

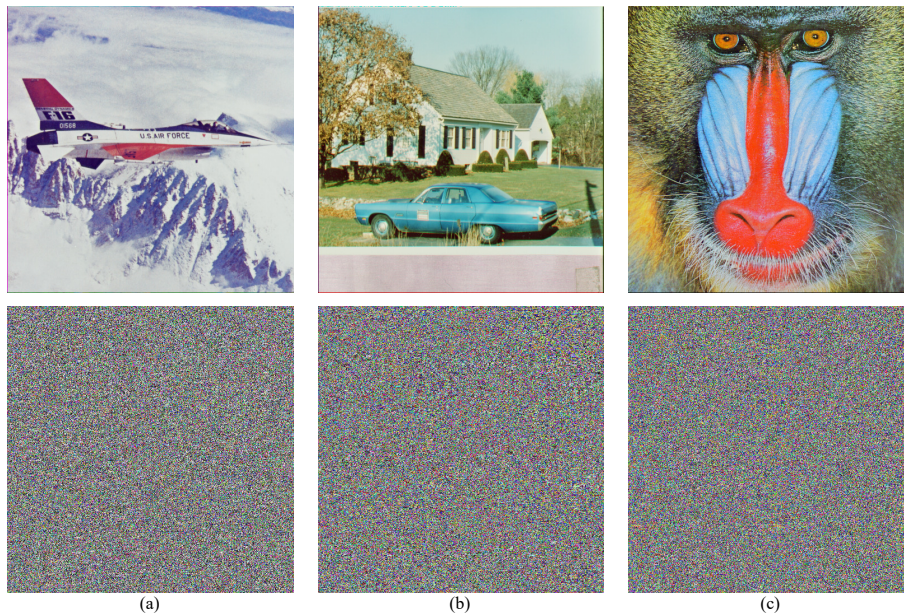


Figure 4. Encryption results. (a) is Jetplane and its encryption image. (b) is House and its encryption image. (c) is Baboon and its encryption image.

4.2 Histogram Analysis

From the perspective of ciphertext histogram, they tend to be uniform, balance the frequency of each pixel value, and have the capability to resist statistical attacks. The histogram of the original image. The ciphertext is demonstrated in Fig. 5-Fig.8.

We find that the pixels of the original image are not uniformly distributed, which is easy to be attacked by statistical analysis. The pixel values of encrypted images are evenly dispersed, which can resist statistical analysis attacks well and ensure the security of information.

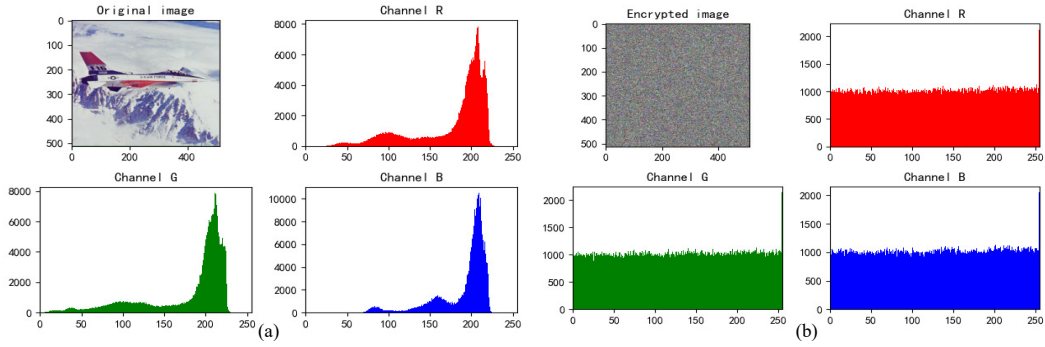


Figure 5. Jetplane's Histogram. (a) is histogram of original Jetplane. (b) is histogram of encrypted Jetplane.

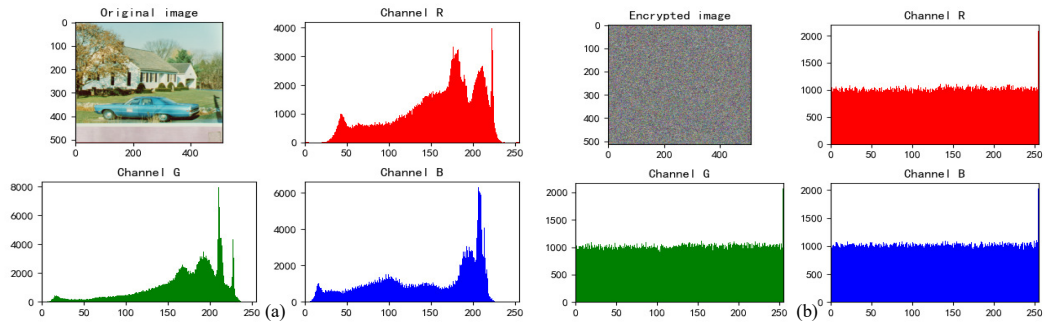


Figure 6. House's Histogram. (a) is histogram of original House. (b) is histogram of encrypted House.

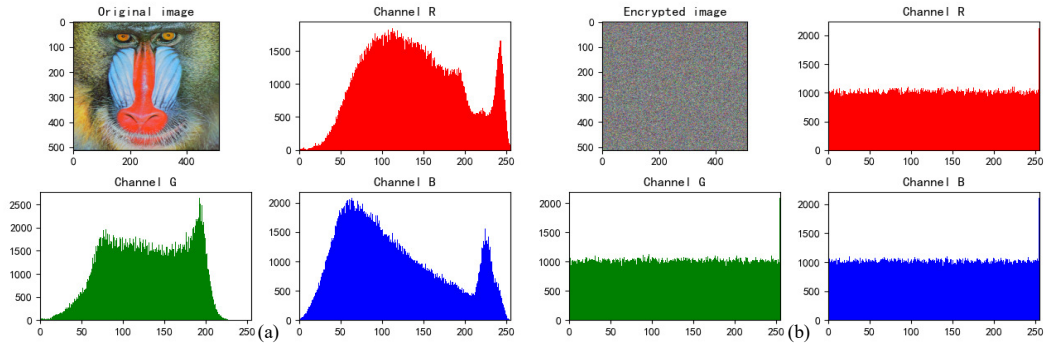


Figure 7. Baboon's Histogram. (a) is histogram of original Baboon. (b) is histogram of encrypted Baboon.

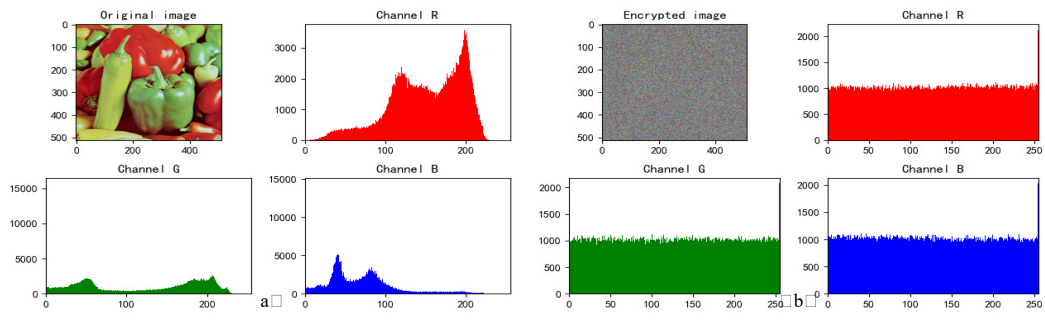


Figure 8. Peppers's Histogram. (a) is histogram of original Peppers. (b) is histogram of encrypted Peppers.

4.3 Information Entrop Analysis

Information entropy is usually used to measure the randomness of a system. In the field of image encryption, information entropy is advantaged to weigh the uncertainty of image information. The more evenly the pixel points of each gray level of the encrypted image R, G, and B are distributed, the better the encryption effect and the stronger the capability to resist external attacks. The formula for calculating information entropy is as follows:

$$H(\alpha) = - \sum_{i=1}^L P(\alpha_i) \log_2 P(\alpha_i) \quad (16)$$

Where $H(\alpha)$ denotes the value of information entropy. The closer its value is to 8, the better the encryption effect is. α_i represents the gray value of the first pixel, and $P(\alpha_i)$ represents the probability of the gray level. Measure the entropy of the three images of Lena, House, Baboon and Peppers after encryption, and the results are illustrated in table 2. Taking Lena image as an example, comparing the encryption method in this paper with the different encryption methods, the results are demonstrated in table 3, which proves the superiority and the security of the encryption method in this paper. The entropy value of the algorithm which put forward in this paper can reach 7.999, which is better than most encryption algorithms.

Table 2. Information Entrop of three channels.

	Jetplane	House	Baboon	Peppers
channel R	7.9991	7.9992	7.9992	7.9992
channel G	7.9991	7.9992	7.9993	7.9993
channel B	7.9989	7.9994	7.9994	7.9994

Table 3. Information Entrop of different encryption.

Information Entrop	Proposed	Ref[28]	Ref[32]	Ref[16]
Jetplane	7.999	*****	*****	*****
House	7.9992	*****	*****	7.9969
Baboon	7.9993	7.9974	*****	*****
Peppers	7.9992	*****	7.9974	7.9851

4.4 Correlation Analysis

Correlation is a measurement standard for calculating the degree of correlation between two variables. Generally speaking, the degree of correlation between adjacent pixels of the image to be encrypted is high commonly, and a third party can infer the characteristics of the surrounding pixels through a pixel. Therefore, image encryption must decrease the correlation as much as possible. We calculate the correlation of encrypted images with using the formula(17). The value range of the correlation coefficient is [-1,1] that the absolute value of the correlation coefficient approaches 0, indicating that the correlation is smaller, and the attack is resisted. The stronger the ability is, the better the effect of image encryption is.

$$R_{y,x} = \frac{\sum_{i=1}^W (y_i - E(y))(x_i - E(x))}{W \sqrt{D(y)} \sqrt{D(x)}} \quad (17)$$

Where $D(y) = \frac{1}{W} \sum_{i=1}^W (y_i - E(y))^2$, $E(y) = \frac{1}{W} \sum_{i=1}^W y_i$. y and x are the adjacent pixels, and W is the total number of pixels in the image. We chose Lena, House and Baboon as the test images to measure the correlation between the original image and the encrypted image of the three images. Firstly, 3000 couples of pixels are selected for each image, and then the correlations in the horizontal, vertical, and diagonal lines are tested respectively. The test results are shown in Fig. 9-Fig. 11 . and table 4. It can be seen that the correlation of the original image is basically linear, while the distribution of the encrypted image is uniform and disorderly. Through the comparison of the two, we can conclude that the encrypted image is weakly correlated and this methods has sound effects.

4.5 Key Space Analysis

For an algorithm of image encryption, it's trustworthy to have a vast key space. So that external eavesdroppers cannot obtain information through brute force enumeration. The Rubik's Cube encryption scheme based on chaotic mapping has better

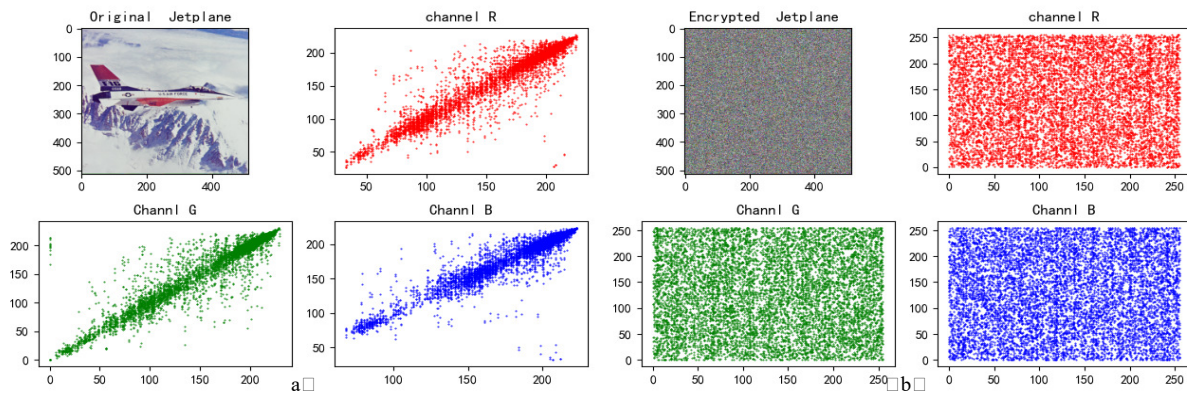


Figure 9. Jetplane's Correlation. (a) is correlation of Jetplane and it's channels. (b) is correlation of encrypted Jetplane and it's channels.

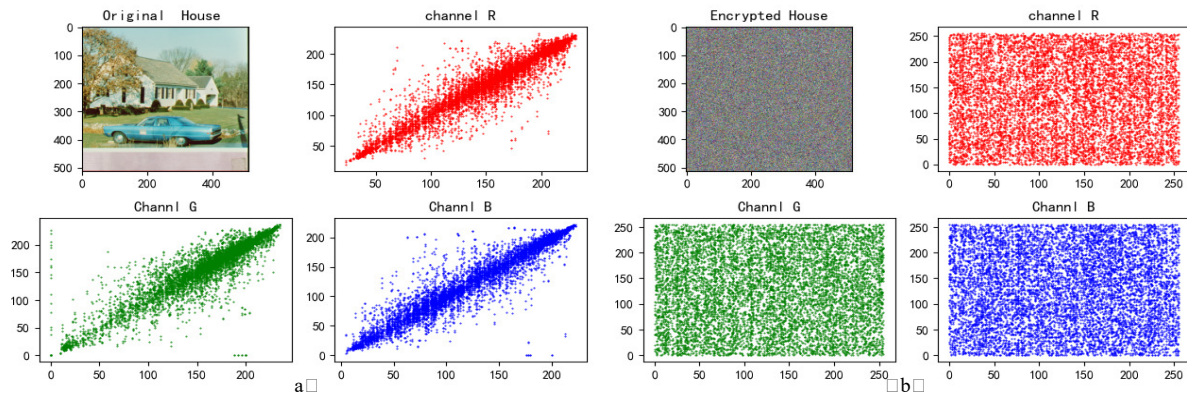


Figure 10. House's Correlation. (a) is correlation of House and it's channels. (b) is correlation of encrypted House and it's channels.

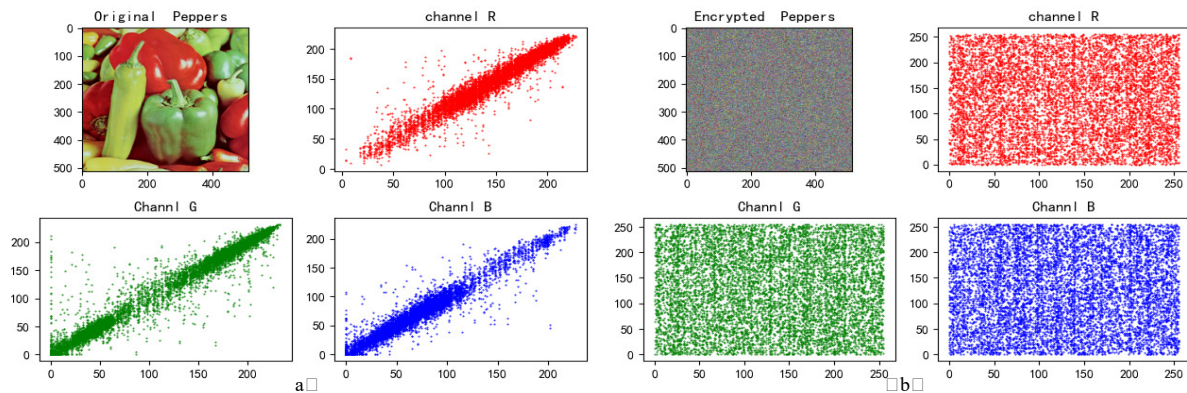


Figure 11. Baboon's Correlation. (a) is correlation of Baboon and it's channels. (b) is correlation of encrypted Baboon and it's channels.

Table 4. Correlation of the original images and encrypted images.

Correlation	Horizontal	Vertical	Diagonal
Original image: Jetplane	0.9685	0.9507	0.9275
Encrypted image: Jetplane	0.0125	0.0134	0.0071
Original image: House	0.9574	0.9620	0.9266
Encrypted image: House	0.0122	0.0098	0.0083
Original image: Baboon	0.9000	0.8349	0.8069
Encrypted image: Baboon	0.0143	0.0103	0.0103

security in some real-time confidential communications, however, the key space of traditional chaotic encryption is limited and there is still a risk of being cracked. The encryption scheme based on alternate quantum walk and Rubik's cube rotation which is put forward in this paper uses the characteristics of alternate quantum walk. While quantum walk are sensitive to the initial state and non-periodic to generate a theoretically infinite space key. Assuming that the initial state of quantum walk is $|\psi_0\rangle$, after the unitary operation of N steps, the final state is $|\psi_N\rangle$:

$$|\psi_N\rangle = \hat{U}^N |\psi_0\rangle \quad (18)$$

The probability of getting a walker at position (y, x) is:

$$P_{Y,X} = \sum |\langle y, x_3 0 | \hat{U}^N | \psi_0 \rangle|^2 + \sum |\langle y, x, 1 | \hat{U}^N | \psi_0 \rangle|^2 \quad (19)$$

Since the possibility of determining an initial state and decomposing a sum of squares is almost zero, there is endless possibility in the key space. In the case that the initial state cannot be obtained, the randomness and unpredictability of the key sequence make the eavesdropper unable to obtain any information, which effectively prevents the information from being cracked and eavesdropped.

4.6 Key Sensitivity Analysis

In order to obtain the key sensitivity of the algorithm, we change a parameter of the key for encryption, and test the change pixel rate NPCR and the average change intensity UACI between it and the correct key. The closer the NPCR is to 99.6094% and the UACI to 33.4635%, the stronger the key sensitivity is. The test results of NPCR and UACI are demonstrated in table 5.

Table 5. NPCR and UACI between encrypted images with different key parameters.

Image	NPCR/%	UACI/%
Lena	99.5991	33.4537
House	99.5670	33.3913
Baboon	99.6181	33.4429
Peppers	99.6073	33.4508
Ref[28]Lena	99.5850	28.6210
Ref[32]Lena	99.6016	33.4753
Ref[16]Lena	99.765	*****

4.7 Analysis of PSNR

PSNR is used to measure the robustness of encrypted images in the field of image encryption. The smaller the value of PSNR is, the greater the difference between the encrypted image and the original image is. Hence, the encryption effect is better. For the original image \mathcal{I} and encrypted image I_{en} . The calculation formula of PSNR is:

$$PSNR = 10 \log_{10} \frac{(2^n - 1)^2 ab}{\sum_{i=1}^a \sum_{j=1}^b (I_{en}(i, j) - \mathcal{I}(i, j))^2} \quad (20)$$

Where a is the width of image, b is the height of the image, and n is the number of pixels. We tested the PSNR values of Lena, House, Baboon, and House, and the test results are shown in table VI below. The test results indicate that encryption method which put forward has better robustness.

Table 6. PSNR of three channels.

PSNR	Jetplane	House	Baboon	Peppers
channel R	8.206	8.713	8.766	9.127
channel G	7.915	8.348	9.226	7.65
channel B	8.006	8.356	8.356	7.648

5 Summary and Prospect

Based on alternate quantum walk and Rubik's cube transform, this paper has put forward a novel color image encryption scheme. The core algorithm of this scheme is to generate random sequence through quantum random walk, extract image pixels to form a third-order Rubik's Cube. Then we control rotation of Rubik's Cube by using random sequences to realize image scrambling. Through experiments, it is found that proposed scheme has a sound encryption effect. The histogram of encrypted image is evenly distributed, the entropy value is about 7.999, the degree of correlation is low, so it can effectively resist statistical attacks. The algorithm has a vast key space and strong key sensitivity, which can effectively resist brute force attacks. The NPCR of encrypted images is around 99.5978%, and the UACI is around 33.4317%, which can effectively resist differential attacks. The PSNR of the encrypted image is low, and it has better robustness.

Author contributions statement

J.Z. and T.Z conceived the scheme, T.Z and J.J conducted the experiment(s), H.M, J.J and T.F analysed the results. All authors reviewed the manuscript.

References

1. Ma Y, Li N, Zhang W, Wang S, Ma H. Image encryption scheme based on alternate quantum walks and discrete cosine transform[J]. *Optics Express*, 2021, 29(18): 28338-28351.
2. Xi S, Wang X, Song L, Zhu Z, Zhu B, Huang S, Yu N, Wang H. Experimental study on optical image encryption with asymmetric double random phase and computer-generated hologram[J]. *Optics express*, 2017, 25(7): 8212-8222.
3. Su Y, Tang C, Gao G, Gu F, Lei Z, Tang S. Optical encryption scheme for multiple color images using complete ternary tree structure[J]. *Optics and Lasers in Engineering*, 2017, 98(nov.):46-55.
4. Tao S, Tang C, Shen Y, Lei Z. Optical image encryption based on biometric keys and singular value decomposition[J]. *Applied optics*, 2020, 59(8): 2422-2430.
5. Fu C, Chen J J, Zou H, Meng W H, Zhan Y F, Yu Y W. A chaos-based digital image encryption scheme with an improved diffusion strategy[J]. *Optics Express*, 2012, 20(3):2363-78.
6. Liansheng S, Bei Z, Xiaojuan N, Ailing T. Optical multiple-image encryption based on the chaotic structured phase masks under the illumination of a vortex beam in the gyrator domain[J]. *Optics Express*, 2016, 24(1): 499-515.
7. Wu T, Zhang C, Chen Y, Cui M, Huang H, Zhang Z, Wen H, Zhao X, Qiu K. Compressive sensing chaotic encryption algorithms for OFDM-PON data transmission[J]. *Optics Express*, 2021, 29(3): 3669-3684.
8. Sui L, Duan K, Liang J, Hei X. Asymmetric double-image encryption based on cascaded discrete fractional random transform and logistic maps[J]. *Optics express*, 2014, 22(9): 10605-10621.
9. Zhong Z, Qin H, Liu L, Zhang Y, Shan M. Silhouette-free image encryption using interference in the multiple-parameter fractional Fourier transform domain[J]. *Optics express*, 2017, 25(6): 6974-6982.
10. Tao R, Xin Y, Wang Y. Double image encryption based on random phase encoding in the fractional Fourier domain[J]. *Optics Express*, 2007, 15(24): 16067-16079.
11. Shi X, Zhao D. Color image hiding based on the phase retrieval technique and Arnold transform[J]. *Applied optics*, 2011, 50(14): 2134-2139.
12. Chen W, Quan C, Tay C J. Optical color image encryption based on Arnold transform and interference method[J]. *Optics communications*, 2009, 282(18): 3680-3685.
13. Wu L, Zhang J, Deng W, D He. Arnold transformation algorithm and anti-Arnold transformation algorithm[C]//2009 first international conference on information science and engineering. IEEE, 2009: 1164-1167.

14. Liu Z, Chen H, Liu T, Li P, Xu L, Dai J, Liu S. Image encryption by using gyrator transform and Arnold transform[J]. *Journal of Electronic Imaging*, 2011, 20(1): 013020.
15. Subramanyan B, Chhabria V M, Babu T G S. Image encryption based on AES key expansion[C]//2011 Second International Conference on Emerging Applications of Information Technology. IEEE, 2011: 217-220.
16. Zhang Q, Ding Q. Digital image encryption based on advanced encryption standard (aes)[C]//2015 Fifth International Conference on Instrumentation and Measurement, Computer, Communication and Control (IMCCC). IEEE, 2015: 1218-1221.
17. Singh A, Agarwal P, Chand M. Image encryption and analysis using dynamic AES[C]//2019 5th International Conference on Optimization and Applications (ICOA). IEEE, 2019: 1-6.
18. Arab A, Rostami M J, Ghavami B. An image encryption method based on chaos system and AES algorithm[J]. *The Journal of Supercomputing*, 2019, 75(10): 6663-6682.
19. Wang Y N, Song Z Y, Ma Y L, Hua N, Ma H Y. Color image encryption algorithm based on DNA coding and alternating quantum random walk[J/OL]. *Acta Physica Sinica*:1-21[2021-10-05].
20. Wang X, Liu C. A novel and effective image encryption algorithm based on chaos and DNA encoding[J]. *Multimedia Tools and Applications*, 2017, 76(5): 6229.
21. Chai X, Chen Y, Broyde L. A novel chaos-based image encryption algorithm using DNA sequence operations[J]. *Optics and Lasers in engineering*, 2017, 88: 197-213.
22. Enayatifar R, Abdullah A H, Isnin I F. Chaos-based image encryption using a hybrid genetic algorithm and a DNA sequence[J]. *Optics and Lasers in Engineering*, 2014, 56: 83-93.
23. Liu H, Wang X. Image encryption using DNA complementary rule and chaotic maps[J]. *Applied Soft Computing*, 2012, 12(5): 1457-1466.
24. Wang X Y, Zhang Y Q, Bao X M. A novel chaotic image encryption scheme using DNA sequence operations[J]. *Optics and Lasers in Engineering*, 2015, 73: 53-61.
25. Cao Y , Gao F , Li D D , et al. Side information -driven quantum composite control for protecting a qubit. 2019.
26. Hong-Yang M, Peng-Ao X, Chang-heng S, Li-bo C, Jia-xin L, Qiong P. Quantum private query based on stable error correcting code in the case of noise[J]. *International Journal of Theoretical Physics*, 2019, 58(12): 4241-4248.
27. Pei-Geng Zhong, Chuang Li, Yan Wang, Jie Song, Shu-Tian Liu, Yong-Yuan Jiang, Yan Xia. Quantum phase transitions triggered by a four-level atomic system in dissipative environments[J]. *Physical Review A*. 2019(4)
28. Ma H, He Z, Xu P, Dong Y, Fan X. A Quantum Richardson–Lucy image restoration algorithm based on controlled rotation operation and Hamiltonian evolution[J]. *Quantum Information Processing*, 2020, 19(8): 1-14.
29. F Gao, SJ Qin, W Huang, QY Wen. Quantum private query: A new kind of practical quantum cryptographic protocol[J]. *Science China*, 2019.
30. Xu P, He Z, Qiu T, Ma H. Quantum image processing algorithm using edge extraction based on Kirsch operator[J]. *Optics express*, 2020, 28(9): 12508-12517.
31. Man Zhang, Lan Zhou, Wei Zhong, Yu-Bo Sheng. Direct measurement of the concurrence of hybrid entangled state based on parity check measurements[J]. *Chinese Physics B*, 2019.
32. Ma Y, Ma H, Chu P. Demonstration of Quantum Image Edge Extration Enhancement Through Improved Sobel Operator[J]. *IEEE Access*, 2020, 8: 210277-210285.
33. Liu F, Zhang X, Xu P A, He Z X, Ma H Y. A Quantum Dialogue Protocol in Discrete-time Quantum Walk Based on Hyperentangled States[J]. *International Journal of Theoretical Physics*, 2020, 59(11): 3491-3507.
34. Ryan C A, Laforest M, Boileau J C, Laflamme R. Experimental implementation of a discrete-time quantum random walk on an NMR quantum-information processor[J]. *Physical Review A*, 2005, 72(6): 062317.
35. Panahiyan S, Fritzsche S. Controlling quantum random walk with a step-dependent coin[J]. *New Journal of Physics*, 2018, 20(8): 083028.
36. Summy G, Wimberger S. Quantum random walk of a Bose-Einstein condensate in momentum space[J]. *Physical Review A*, 2016, 93(2): 023638.
37. Kemp G, Sinayskiy I, Petruccione F. Lazy open quantum walks[J]. *Physical Review A*, 2020, 102(1): 012220.

38. Abd-El-Atty B, Iliyasu A M, Alanezi A, El-latif A. Optical image encryption based on quantum walks[J]. *Optics and Lasers in Engineering*, 2021, 138: 106403.
39. Abdullatif A A, Abdullatif F A, Naji S A. An enhanced hybrid image encryption algorithm using Rubik's cube and dynamic DNA encoding techniques[J]. *Periodicals of Engineering and Natural Sciences (PEN)*, 2019, 7(4): 1607-1617.
40. Zhang L, Tian X, Xia S. A scrambling algorithm of image encryption based on Rubik's cube rotation and logistic sequence[C]//2011 International conference on multimedia and signal processing. IEEE, 2011, 1: 312-315.
41. Pan P, Pan Y, Wang Z, Wang L. Provably Secure Encryption Schemes With Zero Setup and Linear Speed by Using Rubik's Cubes[J]. *IEEE Access*, 2020, 8: 122251-122258.
42. Loukhaoukha K, Chouinard J Y, Berdai A. A secure image encryption algorithm based on Rubik's cube principle[J]. *Journal of Electrical and Computer Engineering*, 2012, 2012.
43. Vidhya R, Brindha M. A chaos based image encryption algorithm using Rubik's cube and prime factorization process (CIERPF)[J]. *Journal of King Saud University-Computer and Information Sciences*, 2020.
44. Wang X Y, Zhang J J, Zhang F C, Cao G H. New chaotical image encryption algorithm based on Fisher-Yates scrambling and DNA coding[J]. *Chinese Physics B*, 2019, 28(4): 040504.
45. Chen M, Ma G, Tang C, Lei Z. Generalized optical encryption framework based on Shearlets for medical image[J]. *Optics and Lasers in Engineering*, 2020, 128: 106026.
46. Shen Y, Tang C, Xu M, Lei Z. Optical selective encryption based on the FRFCM algorithm and face biometric for the medical image[J]. *Optics & Laser Technology*, 2021, 138: 106911.

Acknowledgements

This work is supported by the National Natural Science Foundation of China (No.11975132,61772295), the Natural Science Foundation of Shandong Province, China (No.ZR2019YQ01), the Project of Shandong Province Higher Education Science and Technology Program(No.J18KZ012), and Shandong Provincial Natural Fund Project(No.ZR2021MF049)